PLOS PATHOGENS

Detailed analysis of antibody responses to SARS-CoV-2 vaccination and infection in macaques

Alexandra C. Willcox[1,2,3], **Kevin Sung**[4], **Meghan E. Garrett**[1,3], **Jared G. Galloway**[4], **Jesse H. Erasmus**[5,6], **Jennifer K. Logue**[7], **David W. Hawman**[8], **Helen Y. Chu**[7], **Kim J. Hasenkrug**[9], **Deborah H. Fuller**[5,10,11], **Frederick A. Matsen IV**[4], **Julie Overbaugh**[1] *

1 Human Biology Division, Fred Hutchinson Cancer Research Center, Seattle, Washington, United States of America, 2 Medical Scientist Training Program, University of Washington, Seattle, Washington, United States of America, 3 Molecular and Cellular Biology Program, University of Washington, Seattle, Washington, United States of America, 4 Public Health Sciences Division, Fred Hutchinson Cancer Research Center, Seattle, Washington, United States of America, 5 Department of Microbiology, University of Washington, Seattle, Washington, United States of America, 6 HDT Bio, Seattle, Washington, United States of America, 7 Department of Medicine, University of Washington, Seattle, Washington, United States of America, 8 Laboratory of Virology, Division of Intramural Research, National Institute of Allergy and Infectious Diseases, National Institutes of Health, Hamilton, Montana, United States of America, 9 Laboratory of Persistent Viral Diseases, Division of Intramural Research, National Institute of Allergy and Infectious Diseases, National Institutes of Health, Hamilton, Montana, United States of America, 10 Infectious Diseases and Translational Medicine, Washington National Primate Research Center, Seattle, Washington, United States of America, 11 Center for Innate Immunity and Immune Disease, University of Washington, Seattle, Washington, United States of America

* joverbau@fredhutch.org

Abstract

Macaques are a commonly used model for studying immunity to human viruses, including for studies of SARS-CoV-2 infection and vaccination. However, it is unknown whether macaque antibody responses resemble the response in humans. To answer this question, we employed a phage-based deep mutational scanning approach (Phage-DMS) to compare which linear epitopes are targeted on the SARS-CoV-2 Spike protein in convalescent humans, convalescent (re-infected) rhesus macaques, mRNA-vaccinated humans, and repRNA-vaccinated pigtail macaques. We also used Phage-DMS to determine antibody escape pathways within each epitope, enabling a granular comparison of antibody binding specificities at the locus level. Overall, we identified some common epitope targets in both macaques and humans, including in the fusion peptide (FP) and stem helix-heptad repeat 2 (SH-H) regions. Differences between groups included a response to epitopes in the N-terminal domain (NTD) and C-terminal domain (CTD) in vaccinated humans but not vaccinated macaques, as well as recognition of a CTD epitope and epitopes flanking the FP in convalescent macaques but not convalescent humans. There was also considerable variability in the escape pathways among individuals within each group. Sera from convalescent macaques showed the least variability in escape overall and converged on a common response with vaccinated humans in the SH-H epitope region, suggesting highly similar antibodies were elicited. Collectively, these findings suggest that the antibody response to SARS-CoV-2 in macaques shares many features with humans, but with substantial

differences in the recognition of certain epitopes and considerable individual variability in antibody escape profiles, suggesting a diverse repertoire of antibodies that can respond to major epitopes in both humans and macaques. Differences in macaque species and exposure type may also contribute to these findings.

Author summary

Non-human primates, including macaques, are considered the best animal model for studying infectious diseases that infect humans. Vaccine candidates for SARS-CoV-2 are first tested in macaques to assess immune responses prior to advancing to human trials, and macaques are also used to model the human immune response to SARS-CoV-2 infection. However, there may be differences in how macaque and human antibodies recognize the SARS-CoV-2 entry protein, Spike. Here we characterized the locations on Spike that are recognized by antibodies from vaccinated or infected macaques and humans. We also made mutations to the viral sequence and assessed how these affected antibody binding, enabling a comparison of antibody binding requirements between macaques and humans at a very precise level. We found that macaques and humans share some responses, but also recognize distinct regions of Spike. We also found that in general, antibodies from different individuals had unique responses to viral mutations, regardless of species. These results will yield a better understanding of how macaque data can be used to inform human immunity to SARS-CoV-2.

Introduction

The COVID-19 pandemic has created a pressing need to understand immunity to SARS-CoV-2, both in the setting of vaccination and infection. This has prompted numerous studies in non-human primates (NHPs), which are considered the most relevant animal model for studying many infectious diseases of humans. Various NHP models have been employed to study the immunogenicity and protective efficacy of SARS-CoV-2 vaccine candidates, with most studies using macaque species including rhesus macaques (*Macaca mulatta*) [1–23], cynomolgus macaques (*Macaca fascicularis*) [8,24–32], and pigtail macaques (*Macaca nemestrina*) [22,33–35]. Some of these models have also been used to study infection and re-infection [35–39]. In the NHP model, studies typically measure virus neutralizing antibody responses to vaccination or infection. However, no study has investigated the fine binding specificities of both neutralizing and non-neutralizing SARS-CoV-2 antibodies in macaques and how they compare to the human responses they are meant to model.

Coronaviruses such as SARS-CoV-2 enter host cells using their Spike glycoprotein, which is composed of trimeric S1 and S2 subunits. Receptor-binding S1 homotrimers protrude out from the surface of the virion like a crown, giving this family of viruses its name, while the fusion-mediating S2 trimers anchor the protein to the viral membrane. On S1, the receptor-binding domain (RBD) of SARS-CoV-2 Spike protein binds to angiotensin-converting enzyme 2 (ACE2) on host cells [40,41]. For subsequent membrane fusion to occur, the Spike protein must be cleaved by host cell proteases at the S1/S2 boundary and at an S2' site located just upstream of the fusion peptide (FP) of S2 [42], leading to substantial conformational changes that likely unmask new epitopes of S2 to immune cells [43].

Antibodies to SARS-CoV-2 Spike protein are especially interesting as a potential correlate of protection, as they have the capacity to block infection and kill infected cells [44–47]. There

has understandably been great interest in studying neutralizing antibodies against the RBD, given that such antibodies can directly block interaction with host cells. While RBD-directed antibodies indeed contribute disproportionately to neutralization [48], the majority of the anti-Spike plasma IgG response in convalescent individuals is directed to epitopes outside of the RBD [49,50]. RBD-directed antibodies are also less likely to maintain activity against future viral strains, given the increasing number of variants of concern that harbor mutations in the RBD and have reduced sensitivity to neutralization by immune plasma [51]. Additionally, growing evidence from studies in humans and animal models indicates that non-neutralizing antibodies play a role in protection [52–54].

Previous studies have used Phage-DMS [55], a tool that combines phage display of linear epitopes with deep mutational scanning, to interrogate the fine binding specificities and escape profiles of binding antibodies against all domains of Spike in infected and vaccinated humans [56,57]. These studies have shown that infection-induced human polyclonal antibodies consistently bind linear epitopes in the FP and stem helix-heptad repeat 2 (SH-H) epitope regions, with patient-to-patient variability in escape profiles [56]. Comparatively, mRNA vaccination induces a broader antibody response across Spike protein with more consistent escape profiles [57].

In this study, we built on this foundation by using Phage-DMS to study the binding and escape profiles of antibodies in repRNA-vaccinated pigtail macaques and convalescent (re-infected) rhesus macaques in comparison to mRNA-vaccinated humans and convalescent humans. Our data reveal broad overlap in some major epitopes targeted by both macaques and humans, though neither vaccinated nor convalescent macaques perfectly model the human response. We also find considerable variability in individuals' antibody escape pathways in most epitope regions in both macaques and humans. The broadest responses were seen in vaccinated humans and re-infected rhesus macaques, groups that also share more concordant escape profiles. These results have implications for the interpretation of COVID-19 macaque research studies.

Results

Four groups were included in this study: vaccinated pigtail macaques, vaccinated humans, convalescent (re-infected) rhesus macaques, and convalescent humans (Table 1). The vaccinated macaques received a replicating mRNA (repRNA) vaccine encoding the full-length wild-type (not pre-fusion stabilized) SARS-CoV-2 A.1 lineage Spike protein formulated with a cationic nanocarrier [35,58]. The vaccine was delivered as a prime-only 25μg (n = 3) or 250μg (n = 6) dose or prime-boost 50μg dose (n = 2), with plasma collected 42 days after the first dose (n = 9) or 14 days after the second dose (n = 2). The vaccinated humans received two

Table 1. Details of samples used in the current study.

Group	Number of samples	Age range (years)	Treatment	Time of sample collection
Vaccinated pigtail macaques	11	3 ½-6	repRNA vaccine encoding full-length SARS-CoV-2 Spike[a]	42 days post 1st dose (prime-only, n = 9) or 14 days post 2nd dose (prime-boost, n = 2)
Vaccinated humans	15	18–55	100μg mRNA vaccine encoding full-length pre-fusion stabilized SARS-CoV-2 Spike (Moderna)	36 days post 1st dose
Convalescent rhesus macaques	12	2 ½-5	Infected twice with SARS-CoV-2 six weeks apart[a]	56 days post 1st infection (14 days post 2nd infection)
Convalescent humans	12	28–52	Naturally infected once with SARS-CoV-2 (mild disease)	Median 67 (IQR 62, 70) days post symptom onset

[a]Within each group of macaques, subgroups received slightly different treatments (described in S1 Table).

doses of the 100μg Moderna mRNA-1273 vaccine encoding the pre-fusion stabilized full-length SARS-CoV-2 A.1 lineage Spike protein and formulated with a lipid nanoparticle. Serum was collected from human vaccinees 36 days after the first dose (7 days after the second dose). The convalescent macaques were depleted of CD4+ T cells, CD8+ T cells, CD4+ and CD8+ T cells, or neither as part of a previous study. They were infected twice with SARS-CoV-2, with infections spaced six weeks apart and serum collected 56 days after the first infection (14 days after the second infection). The T cell depleted animals were not excluded based on a detailed analysis of the humoral response in these macaques, which suggested that neither CD4+ nor CD8+ T cells were critical for the development of anamnestic antibody responses, neutralizing antibodies, or protection from re-infection [39]. The convalescent humans were naturally infected once with SARS-CoV-2 and exhibited mild disease, with a median of 67 days between symptom onset and sample collection. Details of individual participants are available in S1 Table.

Enrichment of wildtype peptides

To compare which regions of Spike protein are recognized by human and macaque antibodies, we examined the enrichment of wildtype peptides by antibodies from each individual (Fig 1A). Broadly speaking, binding was observed in the NTD, CTD, FP, and stem helix-HR2 epitope regions as reported previously in human studies [56,57]. Epitope regions (shown as different colors on Fig 1) were defined as previously [57]: NTD, amino acid 285–305; FP, 805–835; stem helix-HR2 (SH-H), 1135–1170. For the CTD, the bounds of epitope regions were expanded and altered from previous studies based on macaque antibodies recognizing a wider area than previously seen in humans: CTD-N', 526–593; CTD-C', 594–685 (S1A Fig). Several additional epitopes that flank previously-defined regions were also identified in this analysis: pre-FP, 777–804; post-FP, 836–855 (S1B Fig); and HR2, 1171–1204 (S1C Fig). Specific epitope regions can be visualized on the structure of a Spike protein monomer in Fig 1B. In addition
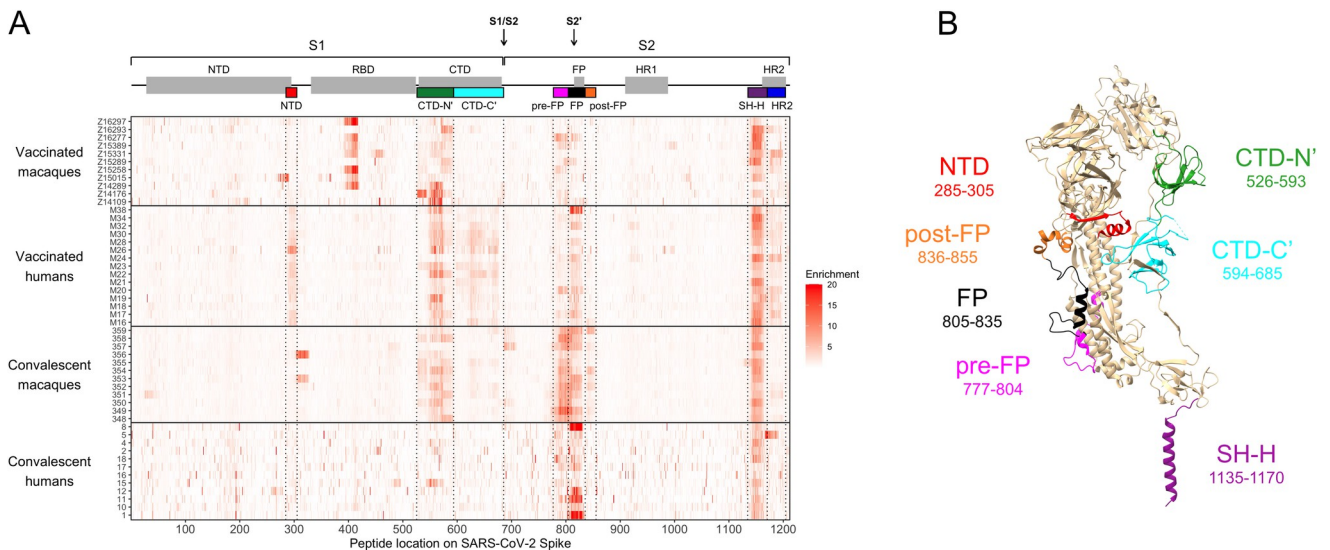
Fig 1. Enrichment of wildtype peptides. (A) The x axis indicates each peptide's location along SARS-CoV-2 Spike protein, and each entry on the y axis is an individual sample. All enrichment values over 20 are plotted as 20 to better show the lower range of the data. Above the heatmap, domains of Spike are shown with grey boxes, with the S1/S2 and S2' cleavage sites indicated with arrows. The epitope regions defined in the current study are shown as colored boxes (from left to right: NTD in red, CTD-N' in green, CTD-C' in cyan, pre-FP in pink, FP in black, post-FP in orange, SH-H in purple, and HR2 in blue). (B) Defined epitope regions shown on a structure of one monomer of SARS-CoV-2 Spike in the pre-fusion conformation (PDB 6XR8 [ref 95]). The amino acid loci spanned by each epitope are listed. The HR2 epitope (AA 1171–1204) could not be resolved on the structure and is not shown.

to these defined regions, we noted that one convalescent rhesus macaque appeared to weakly recognize an epitope at the beginning of the S2 subunit (amino acid 686–710, Fig 1A).

In general, we did not detect responses in the RBD because many epitopes in this region are known to be conformational, and Phage-DMS only has the power to detect epitopes that include linear sequences. Epitopes in the RBD have been extensively detailed elsewhere [59,60]. However, we did detect strong binding to an RBD epitope in some vaccinated pigtail macaques (Fig 1A). This same region was enriched in samples from before vaccination in four of the five pigtail macaques with baseline samples available (S2 Fig). Pre-infection serum from the twelve rhesus macaques did not show such a consistent response, though a few individuals did show strong enrichment of certain peptides (S2 Fig). Because these responses were present prior to vaccination with SARS-CoV-2 Spike or infection with SARS-CoV-2, we did not investigate them further as part of this study. These findings are likely the result of prior exposure to a different coronavirus, as has been documented for human infections.

To quantify differences in the epitopes targeted by different groups, the enrichment of wildtype peptides was summed across each epitope region for every individual. Because the main research question is whether responses in macaques model those in humans, two comparisons were performed: vaccinated macaques vs. vaccinated humans and convalescent macaques vs. convalescent humans (Fig 2).

In concordance with a qualitative assessment of the enrichment heatmap in Fig 1A, vaccinated humans preferentially recognized the following epitope regions compared to vaccinated macaques: NTD (Mann-Whitney $p \leq 0.01$), CTD-C' ($p \leq 0.0001$), and FP ($p \leq 0.05$) (Fig 2A). Meanwhile, convalescent macaques recognized the following epitope regions more than convalescent humans: CTD-N' ($p \leq 0.01$), pre-FP ($p \leq 0.001$), and post-FP ($p \leq 0.01$) (Fig 2B). All groups consistently recognized the SH-H epitope region (Fig 2). While vaccination appeared to induce a stronger response against HR2 than infection (Fig 1A), there were no significant differences in response driven by species (Fig 2). Within each group of macaques (vaccinated and convalescent), subgroups received slightly different treatments (S1 Table), so similar analyses were performed comparing these subgroups; no comparisons were significant at a threshold of $p = 0.05$ (Kruskal-Wallis test, S3 Fig).
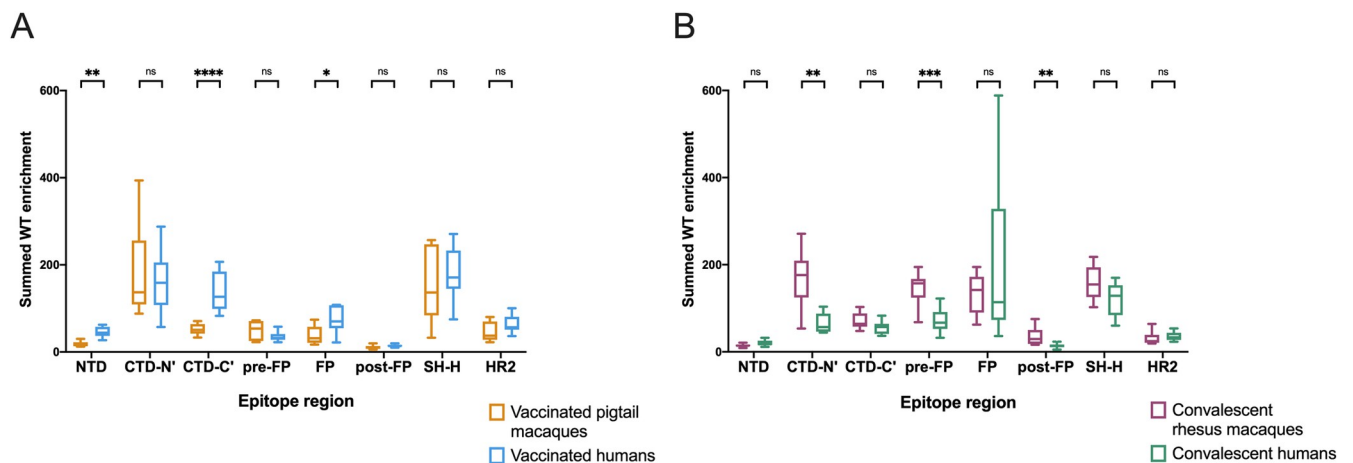
Fig 2. Differences in enrichment of wildtype peptides by group. For each individual, wildtype enrichment values were summed for all peptides within each epitope region. Boxplots summarize the data for all individuals in each sample group. The box represents median and interquartile range (IQR), the lower whisker represents the lowest data point above Q1-1.5IQR, and the upper whisker represents the highest data point below Q3+1.5IQR. (A) compares vaccinated pigtail macaques to vaccinated humans, while (B) compares convalescent rhesus macaques to convalescent humans. Multiple Mann-Whitney U tests were performed, with p values corrected for the number of comparisons in each plot (8) using the Bonferroni-Dunn method. ****, $p \leq 0.0001$; ***, $p \leq 0.001$; **, $p \leq 0.01$; *, $p \leq 0.05$.

https://doi.org/10.1371/journal.ppat.1010155.g002

Taken together, these findings indicate: 1) vaccinated humans were the only group to consistently recognize peptides from both the NTD and CTD-C' epitope regions, which are in close physical proximity to one another (Fig 1B); 2) convalescent humans had a limited response to the CTD-N'; 3) compared to other groups, convalescent macaques had a notably more robust response to regions upstream and downstream of the main FP epitope region; 4) vaccinated macaques did not recognize the FP as strongly as other groups; and 5) vaccination seemed to induce a stronger response against HR2 than infection in both macaques and humans. These findings may also be explained by other differences between the vaccinated and convalescent groups, including the number, dose, and type of exposures.

Defining and comparing escape pathways

To assess differences in the binding characteristics of human and macaque antibodies on a more granular level, we next examined the mutations in Spike that reduced antibody binding in each epitope region of interest. Because the antibody escape pathways for vaccinated humans have been described previously [57], we did not examine the NTD and CTD-C', which are exclusively recognized by this group. Instead, we focused on comparing escape profiles between groups in the following epitope regions: CTD-N', FP, and SH-H. We first represent the data as scaled differential selection values in logo plot form, as commonly shown in previous studies. Importantly, scaled differential selection is highly correlated with peptide binding as measured by competition ELISA [55]. To summarize the data represented by the logo plots by group, summed differential selection values across each epitope region were also calculated. This metric represents the overall magnitude of escape at each locus regardless of the specific amino acid substitution, with negative values indicating a decrease in binding compared to the wildtype amino acid, and positive values indicating enhanced binding (see "Materials and Methods"). Finally, escape similarity scores were calculated between pairs of individuals to quantify similarity in escape profiles (see "Materials and Methods" and S4 Fig).

CTD-N'

Vaccinated macaques, vaccinated humans, and convalescent macaques recognized peptides in the CTD-N' (AA 526–593), whereas convalescent humans generally did not (Fig 2B). Within this epitope region, the individual escape profiles showed notable variability both within and between groups (S5 Fig). For example, across all groups, some individuals showed relatively high sensitivity to mutations between sites 558–567, while others had a response focused more downstream around AA 577–586. There was also substantial variability in which loci in the CTD-N' had the highest relative magnitude of escape, and sometimes even in the directionality of scaled differential selection at a given locus. For example, some individuals had antibodies that bound mutated peptides better than wildtype at AA 555 (e.g., convalescent macaque 353) while others exhibited reduced binding to mutated peptides (e.g., convalescent macaque 358). The same was true for site 560 (e.g., vaccinated humans M24 and M26 exhibited improved and disrupted binding to mutated peptides, respectively).

To summarize the trends observed in the individual findings, we calculated summed differential selection values for each individual at each site and generated boxplots by group (Fig 3A). In addition to the aforementioned regions of escape common to all groups, convalescent macaques also showed considerable escape between AA 529–535, with vaccinated macaques also showing a less consistent response in this area (Figs 3A and S5). The complexity and variability of the escape pathways also prompted us to quantify the similarity in escape between and within groups. Escape similarity scores largely corresponded to areas of high magnitude of escape. Sites with low-magnitude summed differential selection values indicate loci where mutations have no notable impact,
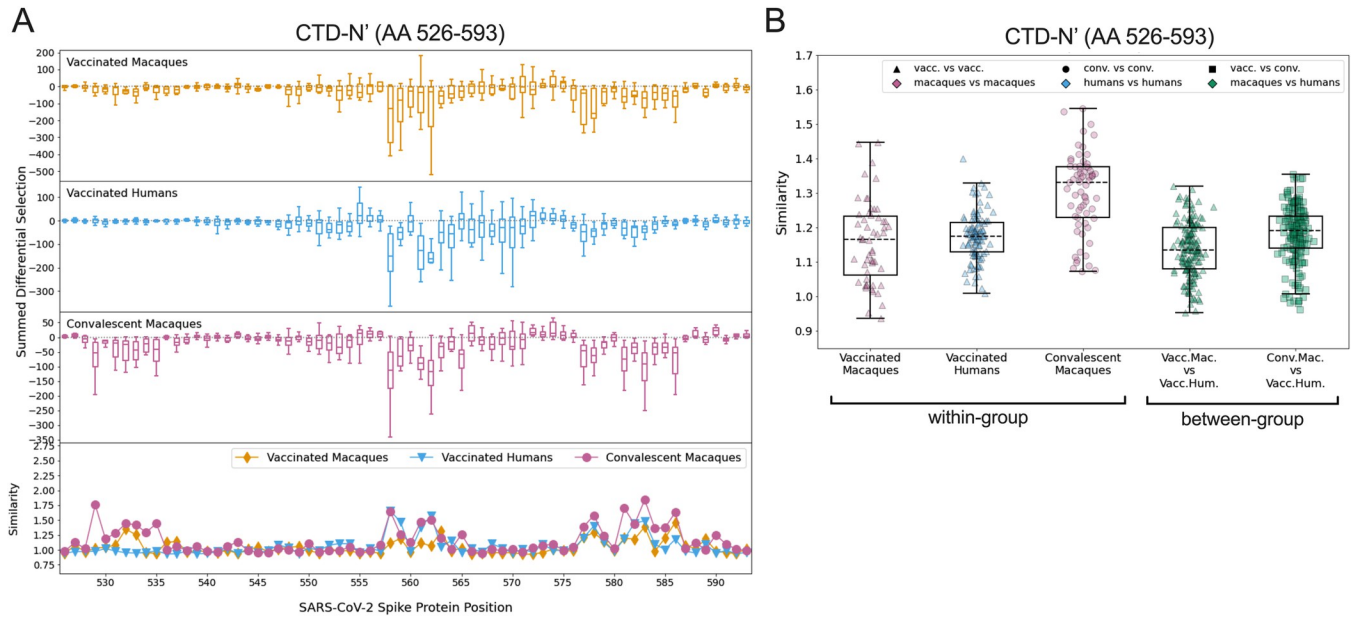
Fig 3. Comparison of escape profiles in the CTD-N'. (A) The top three panels show boxplots depicting the summed differential selection values of all individuals in a group at each locus, with each data point representing a different individual. The box represents median and interquartile range (IQR), the lower whisker represents the lowest data point above Q1-1.5IQR, and the upper whisker represents the highest data point below Q3+1.5IQR. Negative values represent sites where the binding interaction between antibody and peptide was weakened when peptides were mutated, whereas positive values represent enhanced binding. The bottom panel shows the mean escape similarity score for all pairwise comparisons between samples in each group, calculated at every locus. See S4 Fig for a description of the escape similarity score algorithm. (B) Within- and between-group region-wide escape similarity scores, with each point representing a pairwise comparison between two samples. The box represents median and interquartile range (IQR), the lower whisker represents the lowest data point above Q1-1.5IQR, and the upper whisker represents the highest data point below Q3+1.5IQR. The contribution of a site's score to the total escape similarity score is weighted based on its relative contribution to the summed differential selection values across the region. P values are not computed due to lack of independence between data points.

https://doi.org/10.1371/journal.ppat.1010155.g003

and therefore those escape profiles reflect fluctuations in peptide enrichments due to noise, which drives a lower escape similarity score at those sites (Fig 3A, lower panel). At some sites (e.g., 560, as described above), low scores were also the result of some samples showing negative differential selection and others showing positive differential selection, a comparison that was assigned the highest cost in our escape similarity score algorithm.

To test the similarity of escape profiles across the CTD-N' epitope region, escape similarity scores were aggregated across the region and computed both within and between groups. These are shown as boxplots, with each point representing a pairwise comparison between individual samples (Fig 3B). For example, every vaccinated macaque was compared to every other vaccinated macaque (a within-group comparison) and to every vaccinated human (a between-group comparison). We included a comparison of convalescent macaques and vaccinated humans, given visual similarities between their patterns of escape (Fig 3A). Convalescent macaques showed the highest within-group similarity in escape profiles, meaning their escape profiles were more consistent than those of the vaccinated macaques or vaccinated humans (Fig 3B). Between-group escape similarity scores were on par with the within-group scores for the vaccinated macaques and humans, indicating that although there was substantial variability in individual profiles, this was not driven by sample groups.

FP

Escape profiles were examined in the FP epitope region (AA 805–835) for the three groups that showed significant wildtype enrichment in this area: vaccinated humans, convalescent
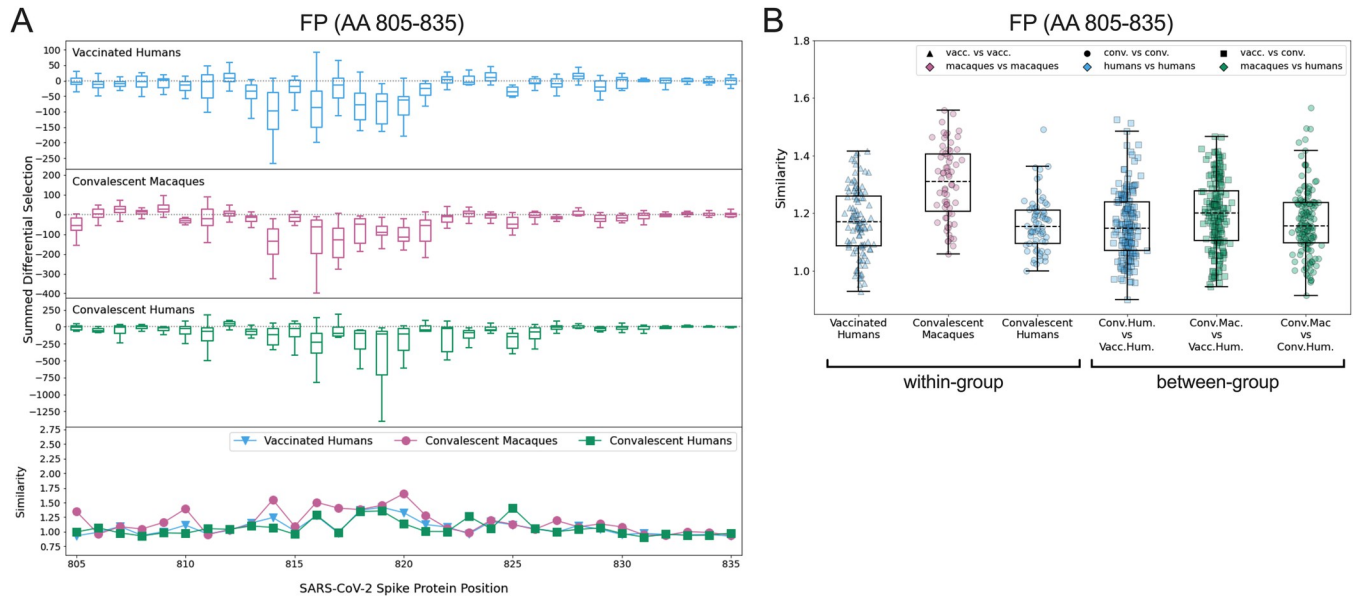
Fig 4. Comparison of escape profiles in the fusion peptide (FP). (A) and (B) Data are shown as described in Fig 3.

https://doi.org/10.1371/journal.ppat.1010155.g004

macaques, and convalescent humans. As in the CTD-N', overall there was variability in individual escape profiles, though the convalescent macaques showed a more consistent pattern of escape than other groups (S6 Fig). Within the FP, most sites of escape fell between AA 811–825 for all groups (Fig 4A). The convalescent macaques again exhibited the highest escape similarity scores (Fig 4B). The median within-group escape similarity scores in the FP were on par with those in the CTD-N' (Fig 3B), indicating approximately equal variability in antibody escape in these epitope regions. The between-group escape similarity scores were generally similar to each other and to the human within-group scores (Fig 4B).

SH-H

All four groups consistently recognized peptides spanning the SH-H epitope region (AA 1135–1170). Major sites of escape were located between AA 1145–1158 for all groups (Fig 5A). The individual logo plots in the SH-H suggested a consistent response among vaccinated humans and convalescent macaques, with more variability in the remaining groups (S7 Fig). This finding is supported by the within-group escape similarity scores for those groups trending higher across the epitope region (Figs 5A lower panel and 5B). The median epitope region-wide escape similarity scores for vaccinated humans and convalescent macaques were also higher in the SH-H than in the CTD-N' or FP, confirming a more concordant response. The median between-group escape similarity score for vaccinated humans and convalescent macaques was on par with their median within-group scores, indicating that the escape profile of a vaccinated human looks as similar to that of a convalescent macaque as it does to another vaccinated human (Fig 5B). The similarity between these two groups was higher than the similarity between convalescent macaques and humans, as well as between vaccinated macaques and humans (Fig 5B). Despite this overall trend, two vaccinated humans had more unique escape profiles (S7 Fig, M26 and M19) and are responsible for a cluster of lower-similarity outlier points (Fig 5B, "Vaccinated Humans" and "Conv. Mac. vs. Vacc. Hum.").

The pairwise comparison between participant 352 (a convalescent macaque) and M21 (a vaccinated human) generated an escape similarity score closest to the median for all
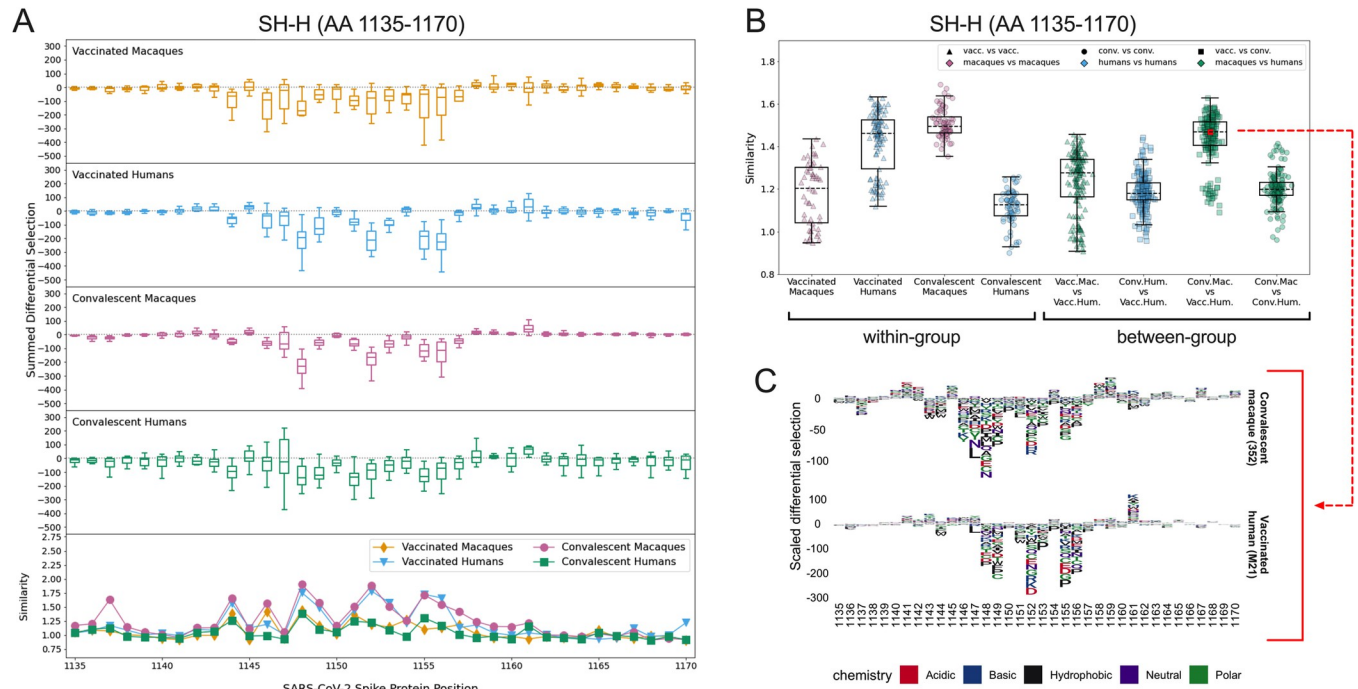
Fig 5. Comparison of escape profiles in the stem helix-HR2 region (SH-H). (A) and (B) Data are shown as described in Fig 3. (C) Logo plots for participant 352 (a convalescent macaque) and M21 (a vaccinated human) showing the effect of specific mutations on antibody binding at each site. The comparison between these samples had an escape similarity score closest to the median value for all pairwise convalescent macaque vs. vaccinated human comparisons and thus can be considered representative of the similarity between these groups. The 352 –M21 comparison is shown in red on (B).

comparisons between these groups. Logo plots for these individuals are shown in Fig 5C as a representative example of the striking between-group similarity. The most consistent sites of escape for both groups were AAs 1148, 1152, 1155, and 1156 (Figs 5A and S7). While some differences exist, there was not nearly as much variability as in the CTD-N' (S5 Fig) and FP (S6 Fig).

Other epitope regions

In addition to the epitope regions described above, the convalescent macaques strongly recognized the pre-FP and post-FP, which were not targeted by human antibody responses (S8 Fig). Escape profiles in the pre-FP appeared highly consistent among individual macaques, with major sites of escape at AAs 795, 798, 800, and 802. Profiles were more variable in the post-FP, likely due in part to low enrichment of wildtype peptides in this epitope region for some individuals (S8 Fig).

Comparison of vaccinated humans and convalescent macaques

It was notable that the vaccinated humans and convalescent macaques showed the most similarity in escape profiles across all epitope regions, most strikingly in the SH-H. Thus, we also asked whether they showed similarity in the epitopes they targeted by comparing the enrichment of wildtype peptides in these groups in each epitope region (S9 Fig). Vaccinated humans recognized the following epitope regions more strongly than convalescent macaques: NTD (Mann-Whitney $p \leq 0.0001$), CTD-C' ($p \leq 0.0001$), and HR2 ($p \leq 0.001$). Convalescent macaques preferentially recognized the pre-FP ($p \leq 0.0001$) and post-FP ($p \leq 0.001$) epitope regions. This suggests some diversity in the epitopes targeted, but similarity of antibody escape patterns within epitopes targeted by both groups.

Discussion

In this study, we aimed to assess whether the antibody binding specificities to SARS-CoV-2 Spike in macaques are a useful model for the human response. Our results indicate important similarities between macaques and humans; for example, both have antibodies that recognize major epitopes in the CTD, FP, and SH-H. However, many differences are also apparent, with some groups showing responses to unique epitopes, such as two physically proximal epitopes in the NTD and CTD that are recognized by antibodies from vaccinated humans but not macaques. Additionally, epitope regions flanking the FP were recognized by antibodies from convalescent macaques, while antibodies from convalescent humans did not recognize the flanking regions but showed a strong response within the FP itself. We found considerable diversity in the pathways of escape between individuals, and this was not specific to either macaques or humans, suggesting a diverse repertoire of antibodies that can respond to the major epitopes in both groups. Overall, these results suggest that macaques and humans share recognition of certain major epitopes. The differences that exist could be due to species (macaque vs. human), but could also be influenced by differences in the specific type and number of exposures to antigen in each group.

Other studies have characterized human monoclonal antibodies against some of the epitopes we report here, many of them with neutralizing or other activities. As previously reported by our group [57], we found that antibodies from vaccinated humans bound peptides spanning a 30 amino acid segment at the C-terminus of the NTD. Interestingly, most if not all neutralizing human mAbs targeting the SARS-CoV-2 NTD to date have been shown to target a single supersite on the "tip" of Spike, distinct from the epitope we detected at the C-terminus [49,61–67]. An NTD mAb with Fc effector function [54], as well as several NTD mAbs that enhance infection in vitro [62,68], also bind sites upstream of the C-terminal epitope. Therefore, future studies are warranted to investigate the function of antibodies binding the new NTD epitope detected by Phage-DMS. In the CTD, we detected broad antibody binding, with vaccinated macaques, vaccinated humans, and convalescent macaques enriching peptides in the CTD-N' epitope region, and vaccinated humans also recognizing peptides spanning the remainder of this domain (CTD-C'). Polyclonal antibodies targeting sites within the CTD-N' and CTD-C' have been isolated from human sera and shown to have neutralizing activity [69]. Interestingly, the neutralizing epitope on the CTD-C' (AA 625–636) [69] is physically adjacent to the NTD epitope we describe (AA 285–305), raising the possibility that a conformational epitope extending to the NTD is recognized by neutralizing antibodies from vaccinated humans. Depleting human serum of FP-binding antibodies reduced its neutralization capacity [70]; these antibodies are of high interest, both due to their potential to block membrane fusion, and given the high sequence conservation among the FPs of diverse coronaviruses [71,72]. We found that convalescent rhesus macaque sera strongly recognized the pre- and post-FP epitope regions, but to our knowledge, functional antibodies against these regions have not been previously described. Finally, the SH-H epitope region we describe is in the stem helix, a region known to be highly conserved across coronaviruses. Broadly neutralizing [73–75] stem helix antibodies have been isolated and suggest an avenue for rational design of a pan-coronavirus vaccine. Interestingly, a mAb raised against the MERS-CoV stem region protected mice against SARS-CoV-2 challenge, despite having no neutralizing activity against SARS-CoV-2 in vitro [76]. The detection of broad antibody binding across Spike supports the continued investigation of non-RBD epitopes, which remain understudied. Some of the epitopes we describe may also be the target of non-neutralizing Fc-effector antibodies [77], and/or antibodies that enhance infection via Fc-independent [68] or Fc-dependent [78] mechanisms. This latter concept may be important in the pathogenesis of COVID-19, though this remains speculative.

Previous work elucidated that pathways of antibody escape to SARS-CoV-2 Spike protein can be quite variable in convalescent humans, with vaccination inducing a more consistent response [57]. In the current study, we found considerable variability in escape profiles in the FP and CTD-N' in both macaques and humans, though the convalescent rhesus macaques had more concordant escape profiles than other groups. Variability in escape patterns suggests that a diversity of antibodies are targeting these epitopes. Intra-species germline diversity in immunoglobulin genes may help explain why individuals with similar exposures often mount distinct responses [79,80]. On the other hand, escape profiles were more consistent in the SH-H, where the responses of convalescent macaques and vaccinated humans appeared to converge. This conservation of response suggests that highly similar antibodies are dominating the antibody repertoire against this epitope. Convergent antibody responses to SARS-CoV-2 have been reported within human populations [81–83], and our findings here suggest that antibodies from different species may also be able to converge on the same "public" antibody repertoires in a functional sense, despite genetic differences. While a shared escape profile among individuals could suggest that viral escape mutations are more likely to emerge on a population level, another factor to consider is the effect of the mutations on viral fitness. Key domains of the S2 subunit (such as the SH-H epitope) have essential functions and high sequence conservation, suggesting a low tolerance for mutation and thus for escape. Indeed, previous work determined that sites of escape identified by Phage-DMS are not typically mutated at a high frequency in circulating strains of SARS-CoV-2 [56].

While our focus was on understanding how macaques and humans respond to a similar exposure (i.e., vaccination or infection), we also noted similarities in response between re-infected macaques and vaccinated humans. These groups both exhibited the broadest recognition across Spike, although the epitope regions they targeted were somewhat different. As described above, these groups also had highly similar antibody escape profiles in the SH-H. The vaccinated humans and re-infected macaques both received two exposures to high doses of antigen. It is plausible that re-exposure directed initially diverse antibodies to converge on a more focused response in both scenarios. While it is known that vaccination and infection induce distinct humoral responses against Spike [57,84,85], our data suggest that a second exposure may generate antibodies that better match the vaccine-induced response.

This study had several limitations. Because the Phage-DMS library displays peptides 31AA in length, discontinuous or conformational epitopes are not readily detected using this method. Additionally, epitopes that may normally be glycosylated are exposed for antibody binding in Phage-DMS. There also are known germline-encoded differences in the properties of immunoglobulin subclasses and Fc receptors between macaques and humans, leading to differences in antibody function that cannot be assayed using Phage-DMS [86]. Additionally, our sample set includes variables that limit our ability to draw conclusions about species-specific (macaque vs. human) differences in antibody response. The vaccinated macaques and humans both received RNA vaccines encoding full-length Spike protein, but there were differences in vaccine technology, including: 1) the use of mRNA in the human vaccine vs. repRNA in the macaque vaccine, 2) the stabilization of Spike in its pre-fusion state in the human vaccine, 3) the dosage and number of doses delivered, and 4) the formulation used to deliver the RNA. Despite these differences, we found commonalities in some of the epitopes targeted by antibodies from both groups. The convalescent rhesus macaques also underwent T cell depletion as part of another study, which may have altered the epitope specifity of their antibodies, although we did not find significant differences between depleted and control animals in our analysis (S3 Fig). Additionally, the convalescent rhesus macaques were experimentally infected twice with high titers of virus, compared to the convalescent humans who were naturally infected once. This important discrepancy could be the reason why the response in re-infected macaques aligned more closely with vaccinated humans than convalescent humans. Studies of

re-infected humans would help address this possibility. Finally, we found pre-existing antibody responses in both groups of macaques. Many of our human samples also likely contain cross-reactive antibodies from prior endemic coronavirus infections. These pre-existing responses are difficult to control for but may have influenced our results.

Our findings suggest that while vaccinated and convalescent macaques and humans share recognition of some major epitopes, each group has a unique antibody binding profile. Antibody escape profiles suggest a diversity of individual responses to most epitopes. Important avenues for future study include comparing macaque and human responses to the RBD and evaluating species differences in antibody function. Continued investigation of immunogenic epitopes in conserved regions of Spike is also warranted to inform the development of immunity that is more robust in the face of viral escape.

Materials and methods

Ethics statement

For the vaccinated pigtail macaques, all procedures were approved by the University of Washington's Institutional Animal Care and Use Committee (IACUC) (IACUC #4266–14). For the convalescent rhesus macaques, all procedures were performed in accordance with Animal Study Proposal RML 2020-046-E approved by the IACUC of Rocky Mountain Laboratories (National Institutes of Health). For the vaccinated humans, all participants provided written informed consent. Because samples were de-identified, this study was approved by the Fred Hutchinson Cancer Research Center Institutional Review Board as non-human subjects research. For the convalescent humans, electronic informed consent was obtained for all participants. This research was approved by the University of Washington Institutional Review Board (IRB number STUDY00000959).

Samples

Vaccinated pigtail macaques. Plasma was collected from 11 pigtail macaques immunized with a replicating RNA (repRNA) vaccine expressing full-length SARS-CoV-2 Spike protein. A subset of these animals was previously described [35]. All animals were housed at the Washington National Primate Research Center (WaNPRC), an accredited facility of the American Association for the Accreditation of Laboratory Animal Care International (AAALAC). Individual macaques received the vaccine by intramuscular injection in either a Lipid InOrganic Nanoparticle (LION) [35] or a Nanostructured Lipid Carrier (NLC) [58] formulation, delivered in a single priming dose of 25μg (n = 3) or 250μg (n = 6) or in a prime-boost regimen with 50μg doses spaced 4 weeks apart (n = 2). All samples were collected 6 weeks post-prime immunization. A subset of these animals also previously received an experimental hepatitis B vaccine as part of another study (n = 5).

Convalescent rhesus macaques. Serum was collected from 12 rhesus macaques housed at the Rocky Mountain Laboratories (National Institutes of Health [NIH]), 14 days after the second of two SARS-CoV-2 infections spaced 42 days apart. The SARS-CoV-2 isolate used for infection was nCoV-WA1-2020 (MN985325.1), which was provided by the Centers for Disease Control and Prevention and propagated as described previously [39]. This isolate came from a COVID-19 patient in Washington state in January 2020 and therefore represents an ancestral strain, prior to the emergence of variants. Prior to infection, macaques were variably depleted of CD4+ T cells, CD8+ T cells, CD4+ and CD8+ T cells, or neither, as part of another study. Details of macaque treatment and regulatory approvals are as published previously [39].

Vaccinated humans. We obtained serum from 15 individuals who received two 100μg doses of the Moderna mRNA-1273 vaccine as part of a phase I clinical trial (NCT04283461)

[87]. Phage-DMS results from these samples were reported previously [57]. Only samples from individuals aged 18–55 years were included in the current study to better match the young age range of the macaques.

Convalescent humans. Plasma was collected from 12 individuals post-mild COVID-19 illness as part of the Hospitalized or Ambulatory Adults with Respiratory Viral Infections (HAARVI) study in Seattle, WA. The date of symptom onset for these individuals ranged from February—March 2020, representing infections with early circulating strains of SARS-CoV-2. Phage-DMS results from these samples were reported previously [56,57]. Again, the sample set was restricted to only include individuals aged 18–55 years to better match other sample groups.

All plasma and sera were heat inactivated at 56˚C for 1 hour prior to use. Full details of all samples are available in Tables 1 and S1.

Phage-DMS, Illumina library preparation and deep sequencing

The experimental protocol was performed exactly as described previously [56]. Briefly, an oligonucleotide pool was synthesized that contains sequences coding for peptides of 31 amino acids that tile along the length of the Wuhan-Hu-1 Spike protein sequence [88] in 1 amino acid increments. For each peptide with the wildtype sequence, 19 variations were included that have a single mutation at the middle amino acid, resulting in a total library size of 24,820 unique sequences. The oligonucleotide pool was cloned into T7 phage, followed by amplification of the phage library; this step was performed twice independently to generate biological duplicate phage libraries. The phage library was incubated with a serum or plasma sample, then bound antibody-phage complexes were immunoprecipitated using Protein A and Protein G Dynabeads (Invitrogen). Bound phage were lysed, and DNA was amplified by PCR and cleaned prior to sequencing on an Illumina MiSeq or HiSeq 2500 with single end reads. Demultiplexing and read alignment were also performed as described previously [57].

Replicate curation

Biological replicates were analyzed in parallel to assess reproducibility of results. For simplicity, results from only one biological replicate are shown and described, with the same figures generated with the second biological replicate available to view online at https://github.com/matsengrp/phage-dms-nhp-analysis. Within each biological replicate, "in-line" technical replicates were run for some samples. In these cases, the technical replicate with the highest mapped read count was selected for analysis.

Wildtype enrichment and defining epitope regions

The enrichment of wildtype peptides was calculated as described previously to quantify the proportion of each peptide in an antibody-selected sample relative to the proportion of that peptide in the input phage library [55]. On enrichment plots, the locus of each peptide is defined by its middle amino acid. Enrichment values of wildtype peptides were summed across epitope regions of interest for statistical comparisons between groups ("Summed WT enrichment" on figures).

Escape profile comparison

The effect of a mutation on antibody-peptide binding was quantified as "differential selection," which is the log fold change in the enrichment of a mutation-containing peptide compared to the wildtype peptide. This number is multiplied by the average of the wildtype peptide

enrichments at that site and its two adjacent sites to get a "scaled differential selection" value, as described previously [57]. The enrichment values of the adjacent wildtype peptides are included in this calculation to make the analysis less susceptible to noise. Negative differential selection values represent reduced binding compared to wildtype, while positive differential selection values indicate that the mutation enhanced binding. "Summed differential selection" is the sum of the 19 scaled differential selection values for all mutations at a site, and gives a sense of the overall magnitude of escape at that site.

The comparison of two escape profiles is quantified by an escape similarity score computed in the framework of an optimal transport problem [89]; this algorithm was described in detail at https://matsengrp.github.io/phippery/esc-prof.html. An overview of the method is shown in S4 Fig. Escape profiles are commonly portrayed as logo plots using scaled differential selection values (S4A Fig). At each site, escape data in logo plot form can instead be represented as binned distributions, with each mutation making some contribution to the total amount of escape at that site based on its scaled differential selection value (S4B Fig). For each site, an optimal transport problem computes the most efficient way to transform one individual's escape distribution into that of a different individual (S4C Fig). The cost to "exchange" amino acid contributions between profiles is based on the similarity between the amino acids being exchanged, as defined by the BLOSUM62 matrix [90]. More "movement" between dissimilar amino acids drives up the total cost of the transport; therefore, a higher cost indicates less similar profiles. Escape similarity scores are the inverse of the total cost of transforming one profile into another. Scores were calculated between pairwise combinations of individuals to compare escape profile variability within and between sample groups.

Protein structure

The structure of a SARS-CoV-2 Spike glycoprotein monomer in the closed state (PDB 6XR8) was examined to visualize epitope regions [91]. Coloring was added using UCSF ChimeraX-1.2.5, developed by the Resource for Biocomputing, Visualization, and Informatics at the University of California, San Francisco, with support from National Institutes of Health R01-GM129325 and the Office of Cyber Infrastructure and Computational Biology, National Institute of Allergy and Infectious Diseases [92].

Statistical analysis and plotting

For comparison of summed wildtype enrichment values across an epitope region between sample groups (Figs 2 and S9), multiple Mann-Whitney U tests were performed, with p values corrected for the number of comparisons in each plot using the Bonferroni-Dunn method. Asterisks represent the following corrected p values: ****, $p \leq 0.0001$; ***, $p \leq 0.001$; **, $p \leq 0.01$; *, $p \leq 0.05$. For comparison of summed wildtype enrichment values between macaque sub-groups (S3 Fig), a Kruskal-Wallis test was used with a significance threshold of $p = 0.05$.

Boxplots are used to summarize summed wildtype enrichment values, summed differential selection values, and similarity scores within a sample group. For all boxplots, the box represents the median and interquartile range (IQR), the lower whisker represents the lowest data point above Q1-1.5IQR, and the upper whisker represents the highest data point below Q3+1.5IQR.

Code and software

All analyses were performed in RStudio version 1.3.1093, Python version 3.6.12, GraphPad Prism version 9.0.1, and the phip-flow and phippery software suite (https://matsengrp.github.io/phippery/). The phip-flow tools perform read alignment using Bowtie2 [93] in a Nextflow

[94] pipeline script. The escape profile comparisons are done with phippery in Python 3.6.12 and depend on the NumPy [95], pandas [96, 97], xarray [98], POT [99], and biopython [100] packages.

Supporting information

S1 Table. Metadata for samples used in this study.
(XLSX)

S1 Fig. Enrichment of wildtype peptides varies by group in newly defined epitope regions.
The locus numbers are shown on the x axis, and each individual is represented in a different color. (A) Wildtype enrichment by group from AA 526–685, spanning the CTD-N' and CTD-C' epitopes. (B) Wildtype enrichment by group from AA 777–855, spanning the pre-FP, FP, and post-FP epitopes. (C) Wildtype enrichment by group from AA 1135–1204, spanning the SH-H and HR2 epitopes.
(TIF)

S2 Fig. Enrichment of wildtype peptides in baseline macaque samples compared to post-vaccination or post-infection samples. The x axis indicates each peptide's location along SARS-CoV-2 Spike protein, and each entry on the y axis is an individual sample. Sample groups are indicated on the left. The same macaques that contributed baseline samples also contributed post-vaccination or post-infection samples. All enrichment values over 20 are plotted as 20 to better show the lower range of the data. Above the heatmap, domains of Spike are shown with grey boxes, with the S1/S2 and S2' cleavage sites indicated with arrows. The epitope regions defined in the current study are shown as colored boxes (from left to right: NTD in red, CTD-N' in green, CTD-C' in cyan, pre-FP in pink, FP in black, post-FP in orange, SH-H in purple, and HR2 in blue).
(TIF)

S3 Fig. Differences in enrichment of wildtype peptides by macaque subgroups. Wildtype enrichment values were summed for all peptides within each region of Spike that showed enrichment. Each point represents an individual macaque. No significant differences were found by Kruskal-Wallis test at a threshold of p = 0.05. LION: Lipid InOrganic Nanoparticle; NLC: Nanostructured Lipid Carrier.
(TIF)

S4 Fig. Use of optimal transport to quantify similarity between amino acid escape profiles.
(A) Profile 1 and 2 show example logo plots for two samples across the same region. Negative scaled differential selection values represent mutations that reduce antibody binding. Amino acids of the same color indicate similar chemistry (e.g., green = polar). (B) At each location (in this example, the boxed site in panel A), the profiles are represented as binned distributions where each bin corresponds to the contribution to escape for an amino acid substitution. (C) The optimal transport solution to transform one profile to the other is computed, where the cost to "exchange" an amino acid contribution in Profile 1 to an amino acid contribution in Profile 2 is derived from the BLOSUM62 matrix. For the purposes of the schematic, the number of dollar signs associated with each line denotes the relative cost of each move (i.e., more dollar signs = more costly = moving between amino acids that are less similar). (D) To quantify similarity between profiles, an escape similarity score is calculated as the inverse of the total cost to perform the transformation. For more details, see https://matsengrp.github.io/phippery/esc-prof.html. Created with BioRender.com.
(TIF)

S5 Fig. Logo plots for all vaccinated macaques, vaccinated humans, and convalescent macaques in the CTD-N' epitope region.
(PNG)

S6 Fig. Logo plots for all vaccinated humans, convalescent macaques, and convalescent humans in the FP epitope region.
(PNG)

S7 Fig. Logo plots for all vaccinated macaques, vaccinated humans, convalescent macaques, and convalescent humans in the SH-H epitope region.
(PNG)

S8 Fig. Logo plots for all convalescent macaques in the pre-FP and post-FP epitope regions.
(PNG)

S9 Fig. Differences in enrichment of wildtype peptides in vaccinated humans and convalescent macaques. As in Fig 2, wildtype enrichment values were summed for each individual for all peptides within each epitope region of Spike. The box represents median and interquartile range (IQR), the lower whisker represents the lowest data point above Q1-1.5IQR, and the upper whisker represents the highest data point below Q3+1.5IQR. Multiple Mann-Whitney U tests were performed, with p values corrected for the number of comparisons (8) using the Bonferroni-Dunn method. ****, $p \leq 0.0001$; ***, $p \leq 0.001$; **, $p \leq 0.01$; *, $p \leq 0.05$.
(TIF)

Acknowledgments

Author Contributions

Conceptualization: Julie Overbaugh.

Data curation: Alexandra C. Willcox, Kevin Sung, Jared G. Galloway.

Formal analysis: Alexandra C. Willcox, Kevin Sung.

Funding acquisition: Jesse H. Erasmus, David W. Hawman, Helen Y. Chu, Kim J. Hasenkrug, Deborah H. Fuller, Frederick A. Matsen IV, Julie Overbaugh.

Investigation: Alexandra C. Willcox, Meghan E. Garrett.

Methodology: Alexandra C. Willcox, Kevin Sung, Meghan E. Garrett, Frederick A. Matsen IV.

Resources: Jesse H. Erasmus, Jennifer K. Logue, David W. Hawman, Helen Y. Chu, Kim J. Hasenkrug, Deborah H. Fuller, Julie Overbaugh.

Software: Kevin Sung, Jared G. Galloway.

Supervision: Frederick A. Matsen IV, Julie Overbaugh.

Validation: Alexandra C. Willcox, Kevin Sung.

Visualization: Alexandra C. Willcox, Kevin Sung.

Writing – original draft: Alexandra C. Willcox, Julie Overbaugh.

Writing – review & editing: Kevin Sung, Meghan E. Garrett, Jared G. Galloway, Jesse H. Erasmus, Jennifer K. Logue, David W. Hawman, Helen Y. Chu, Kim J. Hasenkrug, Deborah H. Fuller, Frederick A. Matsen IV, Julie Overbaugh.

References

1. Corbett KS, Flynn B, Foulds KE, Francica JR, Boyoglu-Barnum S, Werner AP, et al. Evaluation of the mRNA-1273 Vaccine against SARS-CoV-2 in Nonhuman Primates. N Engl J Med. 2020; 383 (16):1544–1555. https://doi.org/10.1056/NEJMoa2024671 PMID: 32722908

2. Vogel AB, Kanevsky I, Che Y, Swanson KA, Muik A, Vormehr M, et al. BNT162b vaccines protect rhesus macaques from SARS-CoV-2. Nature. 2021; 592(7853):283–289. https://doi.org/10.1038/s41586-021-03275-y PMID: 33524990

3. Mercado NB, Zahn R, Wegmann F, Loos C, Chandrashekar A, Yu J, et al. Single-shot Ad26 vaccine protects against SARS-CoV-2 in rhesus macaques. Nature. 2020; 586(7830):583–588. https://doi.org/10.1038/s41586-020-2607-z PMID: 32731257

4. van Doremalen N, Lambe T, Spencer A, Belij-Rammerstorfer S, Purushotham JN, Port JR, et al. ChAdOx1 nCoV-19 vaccine prevents SARS-CoV-2 pneumonia in rhesus macaques. Nature. 2020; 586 (7830):578–582. https://doi.org/10.1038/s41586-020-2608-y PMID: 32731258

5. Gao Q, Bao L, Mao H, Wang L, Xu K, Yang M, et al. Development of an inactivated vaccine candidate for SARS-CoV-2. Science. 2020; 369(6499):77–81. https://doi.org/10.1126/science.abc1932 PMID: 32376603

6. Yu J, Tostanoski LH, Peter L, Mercado NB, McMahan K, Mahrokhian SH, et al. DNA vaccine protection against SARS-CoV-2 in rhesus macaques. Science. 2020; 369(6505):806–811. https://doi.org/10.1126/science.abc6284 PMID: 32434945

7. Yang J, Wang W, Chen Z, Lu S, Yang F, Bi Z, et al. A vaccine targeting the RBD of the S protein of SARS-CoV-2 induces protective immunity. Nature. 2020; 586(7830):572–577. https://doi.org/10.1038/s41586-020-2599-8 PMID: 32726802

8. Wang H, Zhang Y, Huang B, Deng W, Quan Y, Wang W, et al. Development of an Inactivated Vaccine Candidate, BBIBP-CorV, with Potent Protection against SARS-CoV-2. Cell. 2020; 182(3):713–721. e9. https://doi.org/10.1016/j.cell.2020.06.008 PMID: 32778225

9. Feng L, Wang Q, Shan C, Yang C, Feng Y, Wu J, et al. An adenovirus-vectored COVID-19 vaccine confers protection from SARS-COV-2 challenge in rhesus macaques. Nat Commun. 2020; 11:1–11. https://doi.org/10.1038/s41467-019-13993-7 PMID: 31911652

10. Ma X, Zou F, Yu F, Li R, Yuan Y, Zhang Y, et al. Nanoparticle Vaccines Based on the Receptor Binding Domain (RBD) and Heptad Repeat (HR) of SARS-CoV-2 Elicit Robust Protective Immune Responses. Immunity. 2020; 53(6):1315–1330.e9. https://doi.org/10.1016/j.immuni.2020.11.015 PMID: 33275896

11. Sui Y, Li J, Zhang R, Prabhu SK, Andersen H, Venzon D, et al. Protection against SARS-CoV-2 infection by a mucosal vaccine in rhesus macaques. JCI Insight. 2021; 6(10):e148494. https://doi.org/10.1172/jci.insight.148494 PMID: 33908897

12. Harris PE, Brasel T, Massey C, Herst CV, Burkholz S, Lloyd P, et al. A Synthetic Peptide CTL Vaccine Targeting Nucleocapsid Confers Protection from SARS-CoV-2 Challenge in Rhesus Macaques. Vaccines (Basel). 2021; 9(5):520. https://doi.org/10.3390/vaccines9050520 PMID: 34070152

13. Yadav PD, Ella R, Kumar S, Patil DR, Mohandas S, Shete AM, et al. Immunogenicity and protective efficacy of inactivated SARS-CoV-2 vaccine candidate, BBV152 in rhesus macaques. Nat Commun. 2021; 12(1):1386. https://doi.org/10.1038/s41467-021-21639-w PMID: 33654090

14. Garrido C, Curtis AD 2nd, Dennis M, Pathak SH, Gao H, Montefiori D, et al. SARS-CoV-2 vaccines elicit durable immune responses in infant rhesus macaques. Sci Immunol. 2021; 6(60):eabj3684. https://doi.org/10.1126/sciimmunol.abj3684 PMID: 34131024

15. Routhu NK, Cheedarla N, Gangadhara S, Bollimpelli VS, Boddapati AK, Shiferaw A, et al. A modified vaccinia Ankara vector-based vaccine protects macaques from SARS-CoV-2 infection, immune pathology, and dysfunction in the lungs. Immunity. 2021; 54(3):542–556.e9. https://doi.org/10.1016/j.immuni.2021.02.001 PMID: 33631118

16. Li H, Guo L, Zheng H, Li J, Zhao X, Li J, et al. Self-Assembling Nanoparticle Vaccines Displaying the Receptor Binding Domain of SARS-CoV-2 Elicit Robust Protective Immune Responses in Rhesus

Monkeys. Bioconjug Chem. 2021; 32(5):1034–1046. https://doi.org/10.1021/acs.bioconjchem. 1c00208 PMID: 33951913

17. Li Y, Bi Y, Xiao H, Yao Y, Liu X, Hu Z, et al. A novel DNA and protein combination COVID-19 vaccine formulation provides full protection against SARS-CoV-2 in rhesus macaques. Emerg Microbes Infect. 2021; 10(1):342–355. https://doi.org/10.1080/22221751.2021.1887767 PMID: 33555988

18. Arunachalam PS, Walls AC, Golden N, Atyeo C, Fischinger S, Li C, et al. Adjuvanting a subunit COVID-19 vaccine to induce protective immunity. Nature. 2021; 594(7862):253–258. https://doi.org/ 10.1038/s41586-021-03530-2 PMID: 33873199

19. Liang JG, Su D, Song TZ, Zeng Y, Huang W, Wu J, et al. S-Trimer, a COVID-19 subunit vaccine candidate, induces protective immunity in nonhuman primates. Nat Commun. 2021; 12(1):1346. https://doi. org/10.1038/s41467-021-21634-1 PMID: 33649323

20. Luo S, Zhang P, Liu B, Yang C, Liang C, Wang Q, et al. Prime-boost vaccination of mice and rhesus macaques with two novel adenovirus vectored COVID-19 vaccine candidates. Emerg Microbes Infect. 2021; 10(1):1002–1015. https://doi.org/10.1080/22221751.2021.1931466 PMID: 33993845

21. Solforosi L, Kuipers H, Jongeneelen M, Rosendahl Huber SK, van der Lubbe JEM, Dekking L, et al. Immunogenicity and efficacy of one and two doses of Ad26.COV2.S COVID vaccine in adult and aged NHP. J Exp Med. 2021; 218(7):e20202756. https://doi.org/10.1084/jem.20202756 PMID: 33909009

22. Walls AC, Miranda MC, Schafer A, Pham MN, Greaney A, Arunachalam PS, et al. Elicitation of broadly protective sarbecovirus immunity by receptor-binding domain nanoparticle vaccines. Cell. 2021; 184 (21):5432–5447.e16. https://doi.org/10.1016/j.cell.2021.09.015 PMID: 34619077

23. King HAD, Joyce MG, Lakhal-Naouar I, Ahmed A, Cincotta CM, Subra C, et al. Efficacy and breadth of adjuvanted SARS-CoV-2 receptor-binding domain nanoparticle vaccine in macaques. Proc Natl Acad Sci U S A. 2021; 118(38):e2106433118. https://doi.org/10.1073/pnas.2106433118 PMID: 34470866

24. Guebre-Xabier M, Patel N, Tian JH, Zhou B, Maciejewski S, Lam K, et al. NVX-CoV2373 vaccine protects cynomolgus macaque upper and lower airways against SARS-CoV-2 challenge. Vaccine. 2020; 38(50):7892–7896. https://doi.org/10.1016/j.vaccine.2020.10.064 PMID: 33139139

25. Sanchez-Felipe L, Vercruysse T, Sharma S, Ma J, Lemmens V, Van Looveren D, et al. A single-dose live-attenuated YF17D-vectored SARS-CoV-2 vaccine candidate. Nature. 2021; 590(7845):320–325. https://doi.org/10.1038/s41586-020-3035-9 PMID: 33260195

26. Zhang NN, Li XF, Deng YQ, Zhao H, Huang YJ, Yang G, et al. A Thermostable mRNA Vaccine against COVID-19. Cell. 2020; 182(5):1271–1283.e16. https://doi.org/10.1016/j.cell.2020.07.024 PMID: 32795413

27. Li T, Zheng Q, Yu H, Wu D, Xue W, Xiong H, et al. SARS-CoV-2 spike produced in insect cells elicits high neutralization titres in non-human primates. Emerg Microbes Infect. 2020; 9(1):2076–2090. https://doi.org/10.1080/22221751.2020.1821583 PMID: 32897177

28. Brouwer PJM, Brinkkemper M, Maisonnasse P, Dereuddre-Bosquet N, Grobben M, Claireaux M, et al. Two-component spike nanoparticle vaccine protects macaques from SARS-CoV-2 infection. Cell. 2021; 184(5):1188–1200.e19. https://doi.org/10.1016/j.cell.2021.01.035 PMID: 33577765

29. Hong SH, Oh H, Park YW, Kwak HW, Oh EY, Park HJ, et al. Immunization with RBD-P2 and N protects against SARS-CoV-2 in nonhuman primates. Sci Adv. 2021; 7(22):eabg7156. https://doi.org/10. 1126/sciadv.abg7156 PMID: 34049881

30. Sun S, He L, Zhao Z, Gu H, Fang X, Wang T, et al. Recombinant vaccine containing an RBD-Fc fusion induced protection against SARS-CoV-2 in nonhuman primates and mice. Cell Mol Immunol. 2021; 18(4):1070–1073. https://doi.org/10.1038/s41423-021-00658-z PMID: 33731916

31. Capone S, Raggioli A, Gentile M, Battella S, Lahm A, Sommella A, et al. Immunogenicity of a new gorilla adenovirus vaccine candidate for COVID-19. Mol Ther. 2021; 29(8):2412–2423. https://doi.org/ 10.1016/j.ymthe.2021.04.022 PMID: 33895322

32. Kalnin KV, Plitnik T, Kishko M, Zhang J, Zhang D, Beauvais A, et al. Immunogenicity and efficacy of mRNA COVID-19 vaccine MRT5500 in preclinical animal models. NPJ Vaccines. 2021; 6(1):61. https://doi.org/10.1038/s41541-021-00324-5 PMID: 33875658

33. Walls AC, Fiala B, Schafer A, Wrenn S, Pham MN, Murphy M, et al. Elicitation of Potent Neutralizing Antibody Responses by Designed Protein Nanoparticle Vaccines for SARS-CoV-2. Cell. 2020; 183 (5):1367–1382.e17. https://doi.org/10.1016/j.cell.2020.10.043 PMID: 33160446

34. Tan HX, Juno JA, Lee WS, Barber-Axthelm I, Kelly HG, Wragg KM, et al. Immunogenicity of prime-boost protein subunit vaccine strategies against SARS-CoV-2 in mice and macaques. Nat Commun. 2021; 12(1):1403. https://doi.org/10.1038/s41467-021-21665-8 PMID: 33658497

35. Erasmus JH, Khandhar AP, O'Connor MA, Walls AC, Hemann EA, Murapa P, et al. An Alphavirus-derived replicon RNA vaccine induces SARS-CoV-2 neutralizing antibody and T cell responses in

mice and nonhuman primates. Sci Transl Med. 2020; 12(555):eabc9396. https://doi.org/10.1126/scitranslmed.abc9396 PMID: 32690628

36. Hewitt JA, Lutz C, Florence WC, Pitt MLM, Rao S, Rappaport J, et al. ACTIVating Resources for the COVID-19 Pandemic: In Vivo Models for Vaccines and Therapeutics. Cell Host Microbe. 2020; 28 (5):646–659. https://doi.org/10.1016/j.chom.2020.09.016 PMID: 33152279

37. Deng W, Bao L, Liu J, Xiao C, Liu J, Xue J, et al. Primary exposure to SARS-CoV-2 protects against reinfection in rhesus macaques. Science. 2020; 369(6505):818–823. https://doi.org/10.1126/science.abc5343 PMID: 32616673

38. Chandrashekar A, Liu J, Martinot AJ, McMahan K, Mercado NB, Peter L, et al. SARS-CoV-2 infection protects against rechallenge in rhesus macaques. Science. 2020; 369(6505):812–817. https://doi.org/10.1126/science.abc4776 PMID: 32434946

39. Hasenkrug KJ, Feldmann F, Myers L, Santiago ML, Guo K, Barrett BS, et al. Recovery from Acute SARS-CoV-2 Infection and Development of Anamnestic Immune Responses in T Cell-Depleted Rhesus Macaques. mBio. 2021; 12(4):e0150321. https://doi.org/10.1128/mBio.01503-21 PMID: 34311582

40. Walls AC, Park YJ, Tortorici MA, Wall A, McGuire AT, Veesler D. Structure, Function, and Antigenicity of the SARS-CoV-2 Spike Glycoprotein. Cell. 2020; 181(2):281–292.e6. https://doi.org/10.1016/j.cell.2020.02.058 PMID: 32155444

41. Wrapp D, Wang N, Corbett KS, Goldsmith JA, Hsieh CL, Abiona O, et al. Cryo-EM structure of the 2019-nCoV spike in the prefusion conformation. Science. 2020; 367(6483):1260–1263. https://doi.org/10.1126/science.abb2507 PMID: 32075877

42. Li F. Structure, Function, and Evolution of Coronavirus Spike Proteins. Annu Rev Virol. 2016; 3 (1):237–261. https://doi.org/10.1146/annurev-virology-110615-042301 PMID: 27578435

43. Fan X, Cao D, Kong L, Zhang X. Cryo-EM analysis of the post-fusion structure of the SARS-CoV spike glycoprotein. Nat Commun. 2020; 11(1):3618. https://doi.org/10.1038/s41467-020-17371-6 PMID: 32681106

44. Khoury DS, Cromer D, Reynaldi A, Schlub TE, Wheatley AK, Juno JA, et al. Neutralizing antibody levels are highly predictive of immune protection from symptomatic SARS-CoV-2 infection. Nat Med. 2021; 27(7):1205–1211. https://doi.org/10.1038/s41591-021-01377-8 PMID: 34002089

45. Lumley SF, O'Donnell D, Stoesser NE, Matthews PC, Howarth A, Hatch SB, et al. Antibody Status and Incidence of SARS-CoV-2 Infection in Health Care Workers. N Engl J Med. 2021; 384(6):533–540. https://doi.org/10.1056/NEJMoa2034545 PMID: 33369366

46. Corbett KS, Nason MC, Flach B, Gagne M, O' Connell S, Johnston TS, et al. Immune correlates of protection by mRNA-1273 vaccine against SARS-CoV-2 in nonhuman primates. Science. 2021; 373 (6561):eabj0299. https://doi.org/10.1126/science.abj0299 PMID: 34529476

47. Gilbert PB, Montefiori DC, McDermott A, Fong Y, Benkeser DC, Deng W, et al. Immune correlates analysis of the mRNA-1273 COVID-19 vaccine efficacy clinical trial. Science. 2022; 375(6576):43–50. https://doi.org/10.1126/science.abm3425 PMID: 34812653

48. Rogers TF, Zhao F, Huang D, Beutler N, Burns A, He WT, et al. Isolation of potent SARS-CoV-2 neutralizing antibodies and protection from disease in a small animal model. Science. 2020; 369 (6506):956–963. https://doi.org/10.1126/science.abc7520 PMID: 32540903

49. Voss WN, Hou YJ, Johnson NV, Delidakis G, Kim JE, Javanmardi K, et al. Prevalent, protective, and convergent IgG recognition of SARS-CoV-2 non-RBD spike epitopes. Science. 2021; 372 (6546):1108–1112. https://doi.org/10.1126/science.abg5268 PMID: 33947773

50. Greaney AJ, Loes AN, Crawford KHD, Starr TN, Malone KD, Chu HY, et al. Comprehensive mapping of mutations in the SARS-CoV-2 receptor-binding domain that affect recognition by polyclonal human plasma antibodies. Cell Host Microbe. 2021; 29(3):463–476.e6. https://doi.org/10.1016/j.chom.2021.02.003 PMID: 33592168

51. Harvey WT, Carabelli AM, Jackson B, Gupta RK, Thomson EC, Harrison EM, et al. SARS-CoV-2 variants, spike mutations and immune escape. Nat Rev Microbiol. 2021; 19(7):409–424. https://doi.org/10.1038/s41579-021-00573-0 PMID: 34075212

52. Tauzin A, Nayrac M, Benlarbi M, Gong SY, Gasser R, Beaudoin-Bussieres G, et al. A single dose of the SARS-CoV-2 vaccine BNT162b2 elicits Fc-mediated antibody effector functions and T cell responses. Cell Host Microbe. 2021; 29(7):1137–1150.e6. https://doi.org/10.1016/j.chom.2021.06.001 PMID: 34133950

53. Brunet-Ratnasingham E, Anand SP, Gantner P, Dyachenko A, Moquin-Beaudry G, Brassard N, et al. Integrated immunovirological profiling validates plasma SARS-CoV-2 RNA as an early predictor of COVID-19 mortality. Science Advances. 2021; 7(48):eabj5629. https://doi.org/10.1126/sciadv.abj5629 PMID: 34826237

54. Beaudoin-Bussières G, Chen Y, Ullah I, Prévost J, Tolbert WD, Symmes K, et al. A Fc-enhanced NTD-binding non-neutralizing antibody delays virus spread and synergizes with a nAb to protect mice from lethal SARS-CoV-2 infection. Cell Reports. 2022; 38(7):110368. https://doi.org/10.1016/j.celrep.2022.110368 PMID: 35123652

55. Garrett ME, Itell HL, Crawford KHD, Basom R, Bloom JD, Overbaugh J. Phage-DMS: A Comprehensive Method for Fine Mapping of Antibody Epitopes. iScience. 2020; 23(10):101622. https://doi.org/10.1016/j.isci.2020.101622 PMID: 33089110

56. Garrett ME, Galloway J, Chu HY, Itell HL, Stoddard CI, Wolf CR, et al. High-resolution profiling of pathways of escape for SARS-CoV-2 spike-binding antibodies. Cell. 2021; 184(11):2927–2938.e11. https://doi.org/10.1016/j.cell.2021.04.045 PMID: 34010620

57. Garrett ME, Galloway JG, Wolf C, Logue JK, Franko N, Chu HY, et al. Comprehensive characterization of the antibody responses to SARS-CoV-2 Spike protein after infection and/or vaccination. Elife. 2022:e73490. https://doi.org/10.7554/eLife.73490 PMID: 35072628

58. Erasmus JH, Khandhar AP, Guderian J, Granger B, Archer J, Archer M, et al. A Nanostructured Lipid Carrier for Delivery of a Replicating Viral RNA Provides Single, Low-Dose Protection against Zika. Mol Ther. 2018; 26(10):2507–2522. https://doi.org/10.1016/j.ymthe.2018.07.010 PMID: 30078765

59. Yuan M, Liu H, Wu NC, Wilson IA. Recognition of the SARS-CoV-2 receptor binding domain by neutralizing antibodies. Biochem Biophys Res Commun. 2021; 538:192–203. https://doi.org/10.1016/j.bbrc.2020.10.012 PMID: 33069360

60. Niu L, Wittrock KN, Clabaugh GC, Srivastava V, Cho MW. A Structural Landscape of Neutralizing Antibodies Against SARS-CoV-2 Receptor Binding Domain. Front Immunol. 2021; 12:647934. https://doi.org/10.3389/fimmu.2021.647934 PMID: 33995366

61. Chi X, Yan R, Zhang J, Zhang G, Zhang Y, Hao M, et al. A neutralizing human antibody binds to the N-terminal domain of the Spike protein of SARS-CoV-2. Science. 2020; 369(6504):650–655. https://doi.org/10.1126/science.abc6952 PMID: 32571838

62. Li D, Edwards RJ, Manne K, Martinez DR, Schafer A, Alam SM, et al. In vitro and in vivo functions of SARS-CoV-2 infection-enhancing and neutralizing antibodies. Cell. 2021; 184(16):4203–4219.e32. https://doi.org/10.1016/j.cell.2021.06.021 PMID: 34242577

63. Liu L, Wang P, Nair MS, Yu J, Rapp M, Wang Q, et al. Potent neutralizing antibodies against multiple epitopes on SARS-CoV-2 spike. Nature. 2020; 584(7821):450–456. https://doi.org/10.1038/s41586-020-2571-7 PMID: 32698192

64. Wang N, Sun Y, Feng R, Wang Y, Guo Y, Zhang L, et al. Structure-based development of human antibody cocktails against SARS-CoV-2. Cell Res. 2021; 31(1):101–103. https://doi.org/10.1038/s41422-020-00446-w PMID: 33262454

65. Cerutti G, Guo Y, Zhou T, Gorman J, Lee M, Rapp M, et al. Potent SARS-CoV-2 neutralizing antibodies directed against spike N-terminal domain target a single supersite. Cell Host Microbe. 2021; 29 (5):819–833.e7. https://doi.org/10.1016/j.chom.2021.03.005 PMID: 33789084

66. McCallum M, De Marco A, Lempp FA, Tortorici MA, Pinto D, Walls AC, et al. N-terminal domain antigenic mapping reveals a site of vulnerability for SARS-CoV-2. Cell. 2021; 184(9):2332–2347.e16. https://doi.org/10.1016/j.cell.2021.03.028 PMID: 33761326

67. Suryadevara N, Shrihari S, Gilchuk P, VanBlargan LA, Binshtein E, Zost SJ, et al. Neutralizing and protective human monoclonal antibodies recognizing the N-terminal domain of the SARS-CoV-2 spike protein. Cell. 2021; 184(9):2316–2331.e15. https://doi.org/10.1016/j.cell.2021.03.029 PMID: 33773105

68. Liu Y, Soh WT, Kishikawa JI, Hirose M, Nakayama EE, Li S, et al. An infectivity-enhancing site on the SARS-CoV-2 spike protein targeted by antibodies. Cell. 2021; 184(13):3452-3466.e18. https://doi.org/10.1016/j.cell.2021.05.032 PMID: 34139176

69. Li Y, Lai DY, Zhang HN, Jiang HW, Tian X, Ma ML, et al. Linear epitopes of SARS-CoV-2 spike protein elicit neutralizing antibodies in COVID-19 patients. Cell Mol Immunol. 2020; 17(10):1095–1097. https://doi.org/10.1038/s41423-020-00523-5 PMID: 32895485

70. Poh CM, Carissimo G, Wang B, Amrun SN, Lee CY, Chee RS, et al. Two linear epitopes on the SARS-CoV-2 spike protein that elicit neutralising antibodies in COVID-19 patients. Nat Commun. 2020; 11(1):2806. https://doi.org/10.1038/s41467-020-16638-2 PMID: 32483236

71. Tang T, Bidon M, Jaimes JA, Whittaker GR, Daniel S. Coronavirus membrane fusion mechanism offers a potential target for antiviral development. Antiviral Res. 2020; 178:104792. https://doi.org/10.1016/j.antiviral.2020.104792 PMID: 32272173

72. Madu IG, Roth SL, Belouzard S, Whittaker GR. Characterization of a highly conserved domain within the severe acute respiratory syndrome coronavirus spike protein S2 domain with characteristics of a viral fusion peptide. J Virol. 2009; 83(15):7411–7421. https://doi.org/10.1128/JVI.00079-09 PMID: 19439480

73. Zhou P, Yuan M, Song G, Beutler N, Shaabani N, Huang D, et al. A human antibody reveals a conserved site on beta-coronavirus spike proteins and confers protection against SARS-CoV-2 infection. Science Translational Medicine. 2022.

74. Pinto D, Sauer MM, Czudnochowski N, Low JS, Tortorici MA, Housley MP, et al. Broad betacoronavirus neutralization by a stem helix-specific human antibody. Science. 2021; 373(6559):1109–1116. https://doi.org/10.1126/science.abj3321 PMID: 34344823

75. Li W, Chen Y, Prévost J, Ullah I, Lu M, Gong SY, et al. Structural Basis and Mode of Action for Two Broadly Neutralizing Antibodies Against SARS-CoV-2 Emerging Variants of Concern. Cell Reports. 2022; 38(2):110210. https://doi.org/10.1016/j.celrep.2021.110210 PMID: 34971573

76. Hsieh CL, Werner AP, Leist SR, Stevens LJ, Falconer E, Goldsmith JA, et al. Stabilized coronavirus spike stem elicits a broadly protective antibody. Cell Rep. 2021; 37(5):109929. https://doi.org/10.1016/j.celrep.2021.109929 PMID: 34710354

77. Zohar T, Alter G. Dissecting antibody-mediated protection against SARS-CoV-2. Nat Rev Immunol. 2020; 20(7):392–394. https://doi.org/10.1038/s41577-020-0359-5 PMID: 32514035

78. Lee WS, Wheatley AK, Kent SJ, DeKosky BJ. Antibody-dependent enhancement and SARS-CoV-2 vaccines and therapies. Nat Microbiol. 2020; 5(10):1185–1191. https://doi.org/10.1038/s41564-020-00789-5 PMID: 32908214

79. Mikocziova I, Greiff V, Sollid LM. Immunoglobulin germline gene variation and its impact on human disease. Genes Immun. 2021; 22(4):205–217. https://doi.org/10.1038/s41435-021-00145-5 PMID: 34175903

80. Ramesh A, Darko S, Hua A, Overman G, Ransier A, Francica JR, et al. Structure and Diversity of the Rhesus Macaque Immunoglobulin Loci through Multiple De Novo Genome Assemblies. Front Immunol. 2017; 8:1407. https://doi.org/10.3389/fimmu.2017.01407 PMID: 29163486

81. Robbiani DF, Gaebler C, Muecksch F, Lorenzi JCC, Wang Z, Cho A, et al. Convergent antibody responses to SARS-CoV-2 in convalescent individuals. Nature. 2020; 584(7821):437–442. https://doi.org/10.1038/s41586-020-2456-9 PMID: 32555388

82. Chen EC, Gilchuk P, Zost SJ, Suryadevara N, Winkler ES, Cabel CR, et al. Convergent antibody responses to the SARS-CoV-2 spike protein in convalescent and vaccinated individuals. Cell Rep. 2021; 36(8):109604. https://doi.org/10.1016/j.celrep.2021.109604 PMID: 34411541

83. Nielsen SCA, Yang F, Jackson KJL, Hoh RA, Roltgen K, Jean GH, et al. Human B Cell Clonal Expansion and Convergent Antibody Responses to SARS-CoV-2. Cell Host Microbe. 2020; 28(4):516–525. e5. https://doi.org/10.1016/j.chom.2020.09.002 PMID: 32941787

84. Greaney AJ, Loes AN, Gentles LE, Crawford KHD, Starr TN, Malone KD, et al. Antibodies elicited by mRNA-1273 vaccination bind more broadly to the receptor binding domain than do those from SARS-CoV-2 infection. Sci Transl Med. 2021; 13(600):eabi9915. https://doi.org/10.1126/scitranslmed.abi9915 PMID: 34103407

85. Amanat F, Thapa M, Lei T, Ahmed SMS, Adelsberg DC, Carreno JM, et al. SARS-CoV-2 mRNA vaccination induces functionally diverse antibodies to NTD, RBD, and S2. Cell. 2021; 184(15):3936–3948. e10. https://doi.org/10.1016/j.cell.2021.06.005 PMID: 34192529

86. Crowley AR, Ackerman ME. Mind the Gap: How Interspecies Variability in IgG and Its Receptors May Complicate Comparisons of Human and Non-human Primate Effector Function. Front Immunol. 2019; 10:697. https://doi.org/10.3389/fimmu.2019.00697 PMID: 31024542

87. Jackson LA, Anderson EJ, Rouphael NG, Roberts PC, Makhene M, Coler RN, et al. An mRNA Vaccine against SARS-CoV-2—Preliminary Report. N Engl J Med. 2020; 383(20):1920–1931. https://doi.org/10.1056/NEJMoa2022483 PMID: 32663912

88. Wu F, Zhao S, Yu B, Chen YM, Wang W, Song ZG, et al. A new coronavirus associated with human respiratory disease in China. Nature. 2020; 579(7798):265–269. https://doi.org/10.1038/s41586-020-2008-3 PMID: 32015508

89. Monge G. Mémoire sur la théorie des déblais et des remblais. Histoire de l'Académie Royale des Sciences de Paris, avec les Mémoires de Mathématique et de Physique pour la même année. 1781:666–704.

90. Henikoff S, Henikoff JG. Amino acid substitution matrices from protein blocks. Proc Natl Acad Sci U S A. 1992; 89(22):10915–10919. https://doi.org/10.1073/pnas.89.22.10915 PMID: 1438297

91. Cai Y, Zhang J, Xiao T, Peng H, Sterling SM, Walsh RM Jr., et al. Distinct conformational states of SARS-CoV-2 spike protein. Science. 2020; 369(6511):1586–1592. https://doi.org/10.1126/science.abd4251 PMID: 32694201

92. Pettersen EF, Goddard TD, Huang CC, Meng EC, Couch GS, Croll TI, et al. UCSF ChimeraX: Structure visualization for researchers, educators, and developers. Protein Sci. 2021; 30(1):70–82. https://doi.org/10.1002/pro.3943 PMID: 32881101

93. Langmead B, Salzberg SL. Fast gapped-read alignment with Bowtie 2. Nat Methods. 2012; 9(4):357–359. https://doi.org/10.1038/nmeth.1923 PMID: 22388286

94. Di Tommaso P, Chatzou M, Floden EW, Barja PP, Palumbo E, Notredame C. Nextflow enables reproducible computational workflows. Nat Biotechnol. 2017; 35(4):316–319. https://doi.org/10.1038/nbt.3820 PMID: 28398311

95. Harris CR, Millman KJ, van der Walt SJ, Gommers R, Virtanen P, Cournapeau D, et al. Array programming with NumPy. Nature. 2020; 585(7825):357–362. https://doi.org/10.1038/s41586-020-2649-2 PMID: 32939066

96. The pandas development team. pandas-dev/pandas: Pandas. 2020. https://doi.org/10.5281/zenodo.4067057

97. McKinney W. Data Structures for Statistical Computing in Python. Proceedings of the 9th Python in Science Conference. 2010; 445:56–61.

98. Hoyer S, Hamman J. xarray: N-D labeled Arrays and Datasets in Python. Journal of Open Research Software. 2017; 5(1):10.

99. Flamary R, Courty N, Gramfort A, Alaya MZ, Boisbunon A, Chambon S, et al. POT: Python Optimal Transport. JMLR. 2021; 22(78):1–8.

100. Cock PJA, Antao T, Chang JT, Chapman BA, Cox CJ, Dalke A, et al. Biopython: freely available Python tools for computational molecular biology and bioinformatics. Bioinformatics. 2009; 25 (11):1422–1423. https://doi.org/10.1093/bioinformatics/btp163 PMID: 19304878